

Electrical and Optical Analysis of a Spray Coated Transparent Conductive Adhesive for Two-Terminal Silicon Based Tandem Solar Cells

Ulrike Heitmann^{1, a)}, Oliver Höhn¹, Hubert Hauser¹, Sven Kluska¹, Jonas Bartsch¹ and Stefan Janz¹

¹*Fraunhofer Institute for Solar Energy Systems ISE, Heidenhofstrasse 2, 79110 Freiburg, Germany*

^{a)}Corresponding author: ulrike.heitmann@ise.fraunhofer.de

Abstract. This work presents the results of the electrical and optical characterization of a new transparent conductive adhesive (TCA) that combines the techniques of spray pyrolysis and a sol-gel like process. This approach is of particular interest since the adhesive itself forms both the electrical and the mechanical interconnection of the bonded sub-cells. The electrical and optical characterization of the developed TCA shows a minimum connecting resistivity of $17 \Omega\text{cm}^2$ and a simulated reflection at the Si-TCA interface of $\approx 20\%$. By coating both substrate surfaces with a TiO_2 anti reflection coating (ARC), the reflectance at the Si-TCA interface was successfully reduced down to $<5\%$. The efficiency potential of a glued dual junction device was simulated in dependence of the electrical and optical properties of the TCA. The reported values of $17 \Omega\text{cm}^2$ connecting resistivity and 20% reflection limit the device efficiency to 22.3% (71% of the maximum achievable efficiency). Reducing the reflection to below 5% , as practically demonstrated in this paper, allows to increase this value to 25.3% ($>80\%$ of maximum), while additionally reducing the connecting resistivity to $10 \Omega\text{cm}^2$ or $1 \Omega\text{cm}^2$ allows for a further increase to 27.3% and 30.0% , respectively.

INTRODUCTION

Although, silicon-based tandem solar cells have already demonstrated efficiencies up to 33.3% [1], their industrial scale realization still faces the obstacles of costly surface preparations, which are needed for both currently used manufacturing techniques: direct wafer bonding and direct epitaxial growth. One alternative bonding technique that would not require such pre-treatments is using transparent conductive adhesives (TCA). Some recent publications on the topic of TCAs show promising results for the application in tandem solar cells [2,3]. These TCAs usually consist of non-conductive matrices in which conductive particles are embedded that establish the electrical contact. In this publication we show progress with an approach [4] where the matrix material itself connects bottom- and top-cell of the tandem solar cell electrically. The used TCA consists of the precursors for a transparent conductive oxide which are dissolved in an organic solvent. This solution forms at moderate substrate temperatures (100°C) an adhesive layer and subsequent heating to above 300°C leads to calcination and thereby the formation of the TCO. The TCA is applied by spray coating onto both substrates at 100°C which are subsequently joined and laminated in a hot press. The high temperature of the hot press (300°C) leads to the calcination of the adhesive layer while the applied pressure prevents the sample stack from delamination. A variation of the lamination process parameters was carried out and the resulting bonds were electrically and optically characterized.

An optically critical point of such an interconnection is related to reflection losses at the interfaces of the top cell / TCA / bottom solar cell due to the rather low refractive index of the TCA. These losses can be minimized using an anti-reflection coating (ARC) between the semiconductors and the TCA. A TiO_2 based ARC within the bond was demonstrated and its effect was studied using a transfer matrix simulation tool. Based on the measured and simulated results, the theoretical efficiency of a glued tandem solar cell was calculated through 2-diode simulations.

EXPERIMENTAL

Influence of Bonding Process

The developed bonding process consists of spray coating a TCA precursor onto both substrate surfaces and subsequent joining & hot-pressing the stacked substrates in order to enable a mechanical bond and a calcination of the adhesive layer. The spraying of the TCA is done by using a self-built spray coater; the hot pressing is carried out in a Collin PCS II. Through calcination, the gel-like adhesive layer is transformed into a transparent conductive oxide (TCO). This process is similar to a sol-gel process [5] with the difference that the calcination of the layer does not occur while being exposed to a surrounding atmosphere (e.g. air, forming gas etc.) but being enclosed by the two sub-cells of the tandem solar cell. A similar process, but without establishing the electrical connection, is described in [6]. The investigated parameters of the hot-pressing include pressure, overall pressing time and the thickness of the adhesive layer. Due to technical limitations of the used equipment, the temperature during the pressing was limited to 300°C. Temperatures below 300°C were not investigated because differential scanning calorimetry (DSC) analysis of the TCA showed that at lower temperatures the thermal decomposition is not complete. This would mean that the TCA is not transformed into a TCO and therefore not electrically conductive. The bonded substrates consisted of shiny etched, quartered 4" n-type FZ-Si substrates with highly doped (n^{++} , $N_D \approx 1 \times 10^{20} \text{ cm}^{-3}$) TOPCon [7] surfaces and a bulk resistivity of 1 Ωcm . All samples were first coated with a seed layer ($\approx 100 \text{ nm}$) of the TCO deposited by spray pyrolysis [8] to establish the electrical contact to the semiconductors. Table I summarizes the varied parameters.

TABLE I. Overview of the varied bonding process parameters.

Parameter	Variation (high)	Variation (medium)	Variation (low)
Pressure	16 N/cm ²	6 N/cm ²	4 N/cm ²
Pressing time	10 min. preheating + 30 min pressing	10 min preheating + 20 min pressing	10 min. preheating + 10 min pressing
Thickness of TCA	60 iterations of spray coating	40 iterations of spray coating	20 iterations of spray coating

The number of spray iterations (which correlates to the thickness of the adhesive layer) was varied according to Table I. During the hot-pressing, both pressing time and applied pressure have been varied. All parameters were varied based on one initial experiment with all parameters set to intermediate values.

Influence of TiO₂ Anti Reflection Coating

The effect of a TiO₂ based ARC, applied at the semiconductor/TCA interface, was investigated by bonding shiny etched 4" FZ Si substrates, which were sputtered with 100 nm TiO₂. TiO₂ was chosen for its high refractive index of $n_{\text{TiO}_2} = 2.35$. The high refractive index is needed because based on the equation $n_{\text{ARC}} = \sqrt{n_{\text{TCA}} \times n_{\text{Si}}}$ [9], the optimum refractive index of a thin film in between the TCA ($n=1.78$) and silicon ($n=3.63$) would be in the range of 2.54 for the best anti-reflection effect within the relevant wavelength range. To our knowledge, TiO₂ is the closest to this desired refractive index of 2.54 while still being transparent, conductive and readily available. The thickness of the TiO₂ was chosen based on simulation results, which showed the lowest reflection within the relevant wavelength range for TiO₂ films of 100 nm thickness.

The samples were spray coated with the TCA onto the TiO₂ and bonded according to the above described TCA procedure using intermediate pressing parameters (pressure = 5 N/cm², pressing time = 10 min. preheating + 20 min pressing, thickness of TCA = 40 iterations of spray coating). These samples were only characterized for their optical performance (i.e. reflection measurements) and compared to bonded samples without ARC.

RESULTS

The results of the presented work are divided into the electrical analysis and the optical analysis of the developed bonding process. More information on the process development and a structural characterization of the bond can be found in [4].

Electrical Analysis

In order to determine the resistance, which the developed adhesive layer would add to the solar cell structure, the bonded samples were characterized by measuring their I-V characteristics in a 4-point configuration (2 contacts on front- and two contacts on rear side). Beforehand, both front- and rear side of the bonded sample stack were metallized using an evaporated TiPdAg layer. All samples were diced into 5x5 mm² pieces and those from the edge were discarded. The current density was swept between ± 30 mA/cm² and the voltage was measured. The measured I-V curves for one parameter variation, high and low applied pressure, are exemplarily shown in Figure 1.

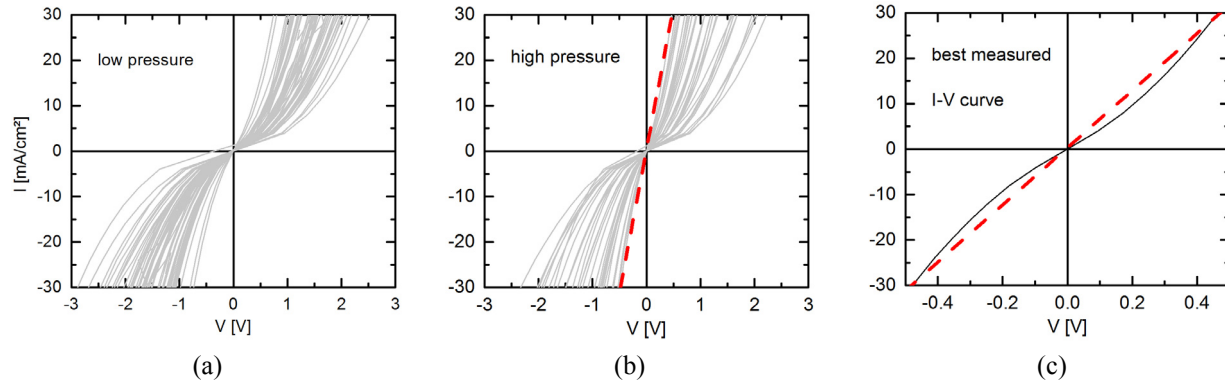


FIGURE 1. Measured I-V curves of samples bonded with low applied pressure (a) and high applied pressure (b). The graph (c) shows the best measured I-V curve, the dashed red line represents a linear fit to the best measured curve.

The only parameter variation that showed a significant effect on the measured I-V curves was the pressure applied during the hot-pressing. Both the variation of pressing time and thickness of the adhesive layer resulted in I-V curves comparable to those recorded for the sample pressed with low applied pressure. Only the sample pressed with high applied pressure showed a steeper trend of the measured I-V curves, which can be seen in Figure 1.

The spread of the curves is caused by the inhomogeneity of the bond layer itself, resulting in different bonded fractions of the cut sample area. The homogeneity of the bond was characterized by Scanning Acoustic Microscopy (SAM). A SAM scan of the samples bonded with varied pressure is shown in Figure 2.

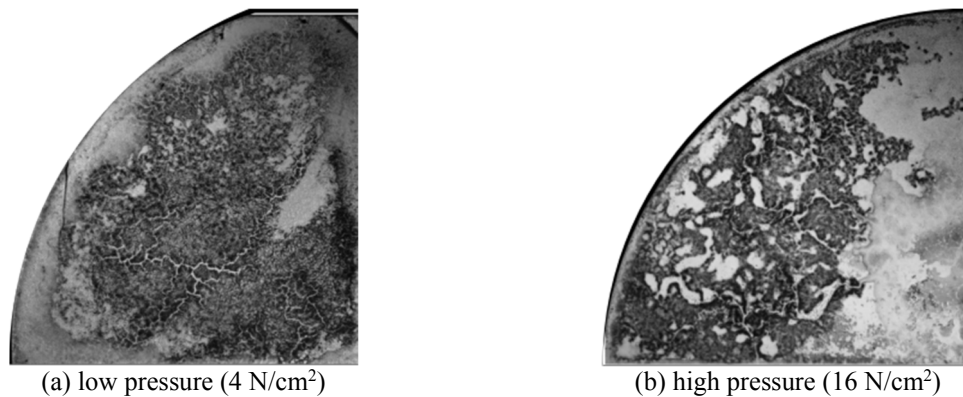


FIGURE 2. SAM scans of samples (1/4 FZ Si substrates) bonded with low pressure (4 N/cm², (a)) and high pressure (16 N/cm², (b)). In general, dark areas correspond to bonded areas while brighter areas show a void in between the two substrates.

By comparing the two SAM scans, it can be seen, that the sample pressed with lower pressure appears to be bonded in a larger area than the sample bonded with high pressure. The structure of the TCA layer of the sample bonded with low pressure shows many fine, brighter channels, which are most likely gas channels that were formed during the heating and calcination of the TCA. The sample bonded with high pressure shows larger bright areas, which appear to be gas trapped in the TCA layer. In between the bright areas however, the bond appears darker and

thereby better bonded. This assumption could explain the fact, that the sample bonded with high pressure shows slightly steeper, more ohmic I-V characteristics.

By linear fitting of the obtained I-V curves, the connecting resistivity was calculated and plotted in a heatmap. Although most of the measured I-V curves do not show a linear trend (except for those with the lowest connecting resistivity), a linear fit of the measured I-V curves still allows a qualitative comparison of the measured curves. The obtained connecting resistivity values were then assembled into a resistivity heatmap of the bonded sample. The heatmap was then superimposed onto the SAM scan in Figure 3 to investigate the correlation between the bonds homogeneity and its connecting resistivity.

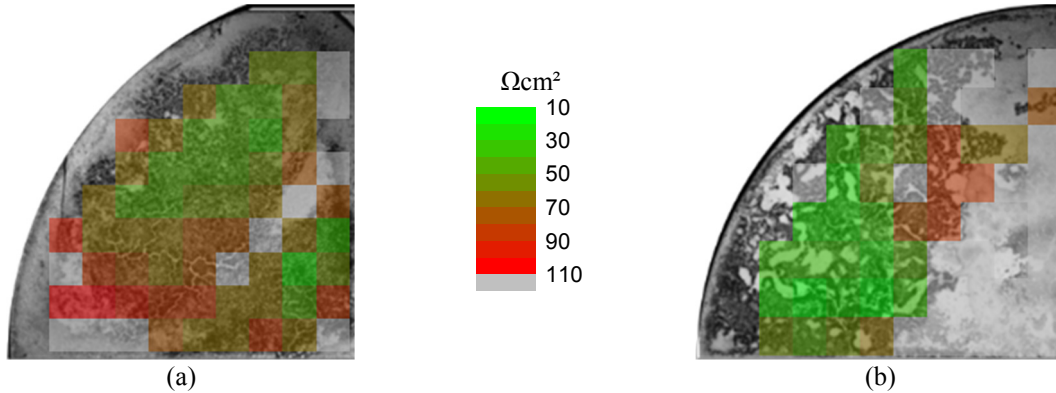


FIGURE 3. SAM scans of bonded samples with the bonds connecting resistivity superimposed as a heatmap. Sample (a) is again the sample pressed with low pressure and (b) was pressed with high pressure.

By comparing the heat maps with the SAM scan, it can be seen, that the connecting resistivity is in general lower in areas that appear darker (= bonded) in the SAM scan. Areas where the SAM scan shows no bond (= bright), showed higher connecting resistivities. Samples which delaminated during the dicing have no color superimposed in the heatmap and samples which stayed bonded but showed connecting resistivities above $110 \Omega\text{cm}^2$ have the color grey superimposed. The heat map also explains why the sample with high pressure bonding process shows lower connecting resistivity, even though the SAM image indicates otherwise. The little bonded area shows comparatively low connecting resistivity at many measured sites, while the connecting resistivity is higher on the sample with low pressure bonding.

By choosing the I-V curve of the best piece cut from the sample pressed with high pressure and performing a linear fit, a lowest connecting resistivity of approximately $17 \Omega\text{cm}^2$ was calculated. The recorded I-V curve and its linear fit are shown in Fig. 1 (c). By further improving the homogeneity of the bond it is expected that this low connecting resistivity will be realizable over the whole sample area in the near future. An optimization of the bonding process is ongoing with the focus set on adapting both temperature and pressure profiles of the hot pressing to the thermal decomposition of the TCA.

Optical Analysis

Apart from a good electrical interconnection, the optical behavior of the bond layer in between the two semiconductors is essential, since all light that is lost due to absorption within the TCA, or reflection at the top cell/TCA/bottom cell interfaces decreases the current generated in the bottom solar cell. A bonded sample, consisting of two $4''$, $1 \Omega\text{cm}$ FZ Si substrates bonded by the previously described intermediate process, was analyzed using a UV-Vis spectrometer. The measured reflection is shown in Figure 4 (b) (black dashed curve). The obtained reflection spectrum of the sample without ARC was fed into a transfer matrix simulation along with literature values for refractive index n and extinction coefficient k of the Si substrates [10]. The TCA refractive index and thickness was then adjusted to replicate the minima and maxima of the measured spectrum as close as possible. The obtained refractive index of the TCA of $n=1.78$ and a layer thickness of $1.3 \mu\text{m}$ agree well with ellipsometry measurements and SEM cross section analysis respectively. This optical model was then changed by assuming the silicon substrates to be of semi-infinite thickness (Figure 5 (a)) in order to simulate the reflection caused only by the inner two silicon/TCA interfaces. The obtained curve is shown in Figure 5 (b). By averaging the

reflection within the relevant wavelength range, an approximate reflection of 20% was determined. This high reflectivity of the TCA/substrate interfaces would strongly affect the performance of a bonded tandem solar cell. We therefore investigated possible anti-reflection coatings, which could be implemented at the TCA/substrate interfaces. A 100 nm TiO_2 thin film was found to be a good candidate for the ARC, as can be seen in the simulated reflection curve in Figure 5 (b) (blue curve).

In order to investigate the effectiveness of the ARC, the same bonding process was applied to a similar pair of samples that were additionally sputter-coated with 100 nm TiO_2 . The measured reflection of the sample including the TiO_2 anti reflection coating (ARC) is also shown in Figure 4 (b) (blue dotted curve). The measured reflection of the sample agrees well with the simulation, showing a reduced reflection. The fact that the measured reflection of the sample with the TiO_2 ARC does not show Fabry-Perot interferences as strong as the simulated results could be due to scattering within the TCA or variations in the TCA's thickness.

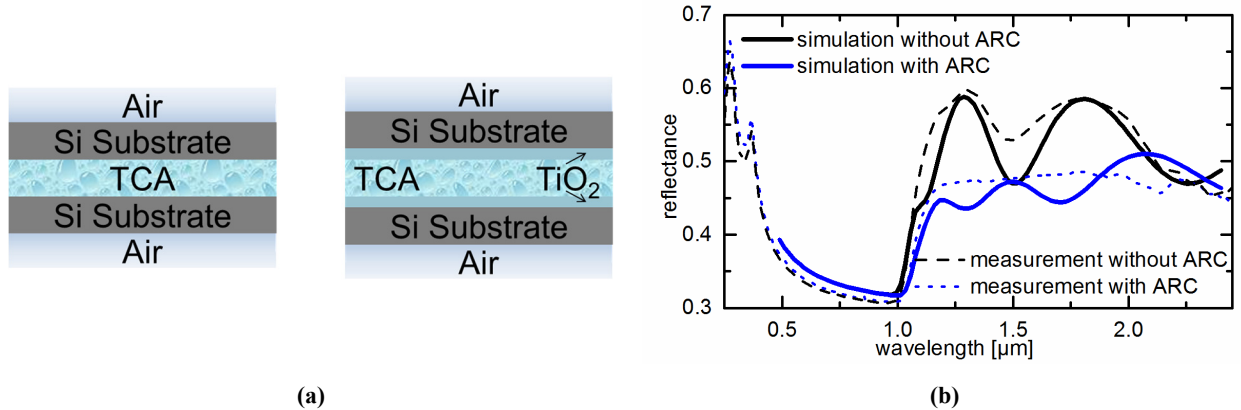


FIGURE 4. The models used for simulating the reflection of the whole sample stack with and without a TiO_2 based anti-reflection coating are shown in (a). The results of the simulation are shown in (b), drawn as a continuous line. The measured reflectance spectra of the samples with and without the ARC are plotted in dashed and dotted lines in (b).

In order to investigate the reflection within the wavelength range, which is relevant for a Si-based tandem solar cell (730-1150 nm), the Si substrates were assumed to be of semi-infinite thickness for another optical simulation (Fig. 5 (a)). This allows us to investigate the internal reflection caused only by the TCA interfaces over the whole relevant wavelength range. The simulation shows that the reflection at the interfaces without the TiO_2 ARC amounts to roughly 20%. The TiO_2 layer successfully reduces the reflection within the relevant wavelength range down to an average of 2.0%. The model together with the results of the simulation is shown in Figure 5.

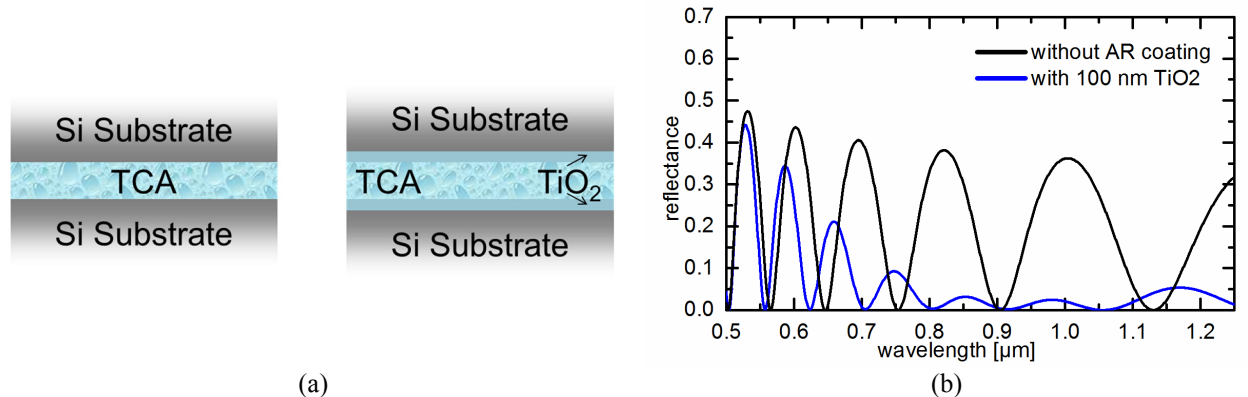


FIGURE 5. The model including the semi-infinite silicon substrates is displayed in (a). The simulation result, showing only the reflection caused by the TCA/Si interface, is shown in (b).

In order to test if the optical behavior of the ARC would be the same in a real device, the top layer in the optical model was changed to semi-infinite GaAs. With GaAs as top layer, the average reflection within the relevant

wavelength range now amounts to 2.3%. For comparison, the simulation results for bonded silicon substrates and silicon bonded to GaAs are shown in Figure 6 (both sample structures include the TiO₂ based ARC at both semiconductor surfaces).

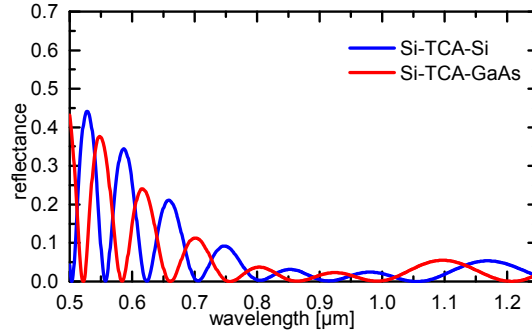


FIGURE 6. Comparison of the simulated reflectance of the TCA/semiconductor interfaces including the TiO₂ based ARC in two different sample structures: silicon glued to silicon and silicon glued to GaAs.

This result shows, that the chosen test structure (Si-Si) for the optical analysis of the ARC is very close to the simulated optical behavior of the real device (Si-GaAs) and therefore well suited for characterization of the optical losses caused by the developed bonding process. The influence of the TiO₂ thin film on the electrical behavior of the bond still has to be investigated, but in literature, thin TiO₂ layers are commonly implemented for example in perovskite based solar cells [11].

ESTIMATED POTENTIAL OF BONDED DEVICE

The two main limiting parameters of the TCA are its series resistance contribution to the final device and the reflection at the TCA/semiconductor interfaces, which directly translates into a current loss in the bottom cell. In order to calculate the efficiency of such a glued tandem solar cell, a two diode model was in a first step adjusted to replicate the published result of a wafer bonded, silicon-based tandem solar cell (three junctions, $\eta = 33.3\%$, [1]). This two diode model thereby includes realistic values for losses due to radiative recombination and a realistic performance of the silicon bottom cell. The model was then changed into a dual junction tandem solar cell model by replacing the two III-V top cells by one III-V top cell with a band gap of $E_{G1}=1.72$ eV and keeping the silicon bottom cell ($E_{G2}=1.12$ eV). The J_{SC} of the tandem cell is 19 mA, the sub cell V_{OC} 's are $V_{OC(top)} = 1.3$ V and $V_{OC(bottom)} = 0.7$ V. A varied series resistance of up to 30 Ωcm^2 , corresponding to the TCA-induced connecting resistivity, was added to the two junctions. The reflection at the TCA-semiconductor interfaces was varied between 0-30% and was assumed to directly translate into a current loss within the bottom solar cell. The resulting efficiencies of a glued tandem solar cell in dependence on the connecting resistivity and reflection caused by the used TCA are shown in Figure 7.

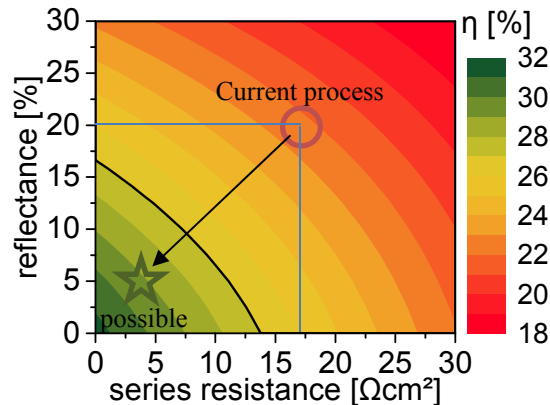


FIGURE 7. Efficiency analysis of a bonded dual junction tandem solar cell as a function of the bond TCA's connecting resistivity (added as series resistance) and the current loss in the bottom cell (caused by the reflection at the interface).

A tandem solar cell bonded with the current TCA (connecting resistivity = $17 \text{ } \Omega\text{cm}^2$ and 20% reflection at the interface) would achieve an efficiency of $\approx 22\%$ (red circle). If a TiO_2 based ARC is implemented, the reflection can be reduced to $<5\%$. If the connecting resistivity can also be brought down to $10 \text{ } \Omega\text{cm}^2$, an efficiency of 27.3%, which is above the current record of a single junction silicon solar cell [12] can be achieved. For connecting resistivities below $1 \text{ } \Omega\text{cm}^2$, efficiencies above 30% are within reach, if the TiO_2 ARC is successfully integrated into the tandem solar cell.

ACKNOWLEDGEMENTS

The authors would like to thank all co-workers at Fraunhofer ISE for their support and input in many valuable discussions. This work has received funding from the European Union's Horizon 2020 research and innovation program within the project SiTaSol under grant agreement No 727497 and from the Federal Ministry for Economic Affairs within the Project SolGelPV (FKZ 0324151A).

REFERENCES

1. R. Cariou et al., [Nature Energy](#) 3 (4), 326-333 (2018).
2. T. R. Klein et al., [ACS Appl. Mater. Interfaces](#) 10 (9), 8086-8091 (2018).
3. S. Yoshidomi et al., [Energy Procedia](#) 60, 116-122 (2014).
4. U. Heitmann et al., Proceedings of the 7th WCPEC, Waikoloa, Hawaii, USA, 2018
5. J-H. Lee and B-O. Park, [Thin Solid Films](#) 426 (1-2), 94-99 (2003).
6. C. J. Barbé et al., [Thin Solid Films](#) 488 (1-2), 153-159 (2005).
7. F. Feldmann et al., [Solar Energy Materials and Solar Cells](#) 120, Part A, 270-274 (2014).
8. M. A. Lucio-Lopez et al., [Solar Energy Materials and Solar Cells](#) 90 (6), 733-741 (2006).
9. H. A. Macleod, *Thin-Film Optical Filters* (Taylor & Francis, Boca Raton, 2010), pp. 107.
10. M. A. Green, [Solar Energy Materials and Solar Cells](#) 92 (11), 1305-1310 (2008).
11. A. Möllmann et al., [Advanced Energy Materials](#) 348, 1801196 (2019).
12. K. Yoshikawa et al., [Nature Energy](#) 2, 17032 (2017).